Smart Rock Technology for Real-time Monitoring of Bridge Scour and Riprap Effectiveness – Design Guidelines and Visualization Tools (Progress Report No. 2)

Contract No: OASRTRS-14-H-MST
(Missouri University of Science and Technology)

Reporting Period: January 1 – March 31, 2015

PI: Genda Chen

Program Manager: Mr. Caesar Singh

Submission Date: April 15, 2015

TABLE OF CONTENTS

EXECUTIVE SUMMARY

In the second quarter of this project, bridge and river data were collected for the design of smart rocks and for the development of design guidelines. The critical flow velocity equation in HEC18 and the riprap sizing equation in HEC23 were used to establish the relationship between the size and density of smart rocks corresponding to their incipient motion. The two equations were applied into two bridges in California (Waddell Creek and Kings Creek) and two bridges in Missouri (US 63 Gasconade River and I-44 Roubidoux Creek). The size of the smart rocks was first determined to meet the requirements for fabrication. The density of the smart rocks was calculated from the analysis of incipient motion derived from the density-size interrelation of smart rocks.

The final design of smart rocks was a sphere of 0.25 m in diameter and 1530 kg/m^3 in density that was determined by multiplying a design factor by the density calculated from the analysis of incipient motion. The design factor was introduced to ensure that the smart rocks would not be washed away at various bridge sites. It is considered as 1.2 for bridge sites with detailed hydraulic analysis and 1.3 for bridge sites with no hydraulic analysis. A gravity-oriented magnet was embedded inside each smart rock so that the orientation of the magnet would be known *in priori* and remained vertical during measurements. When the sensors of a magnetometer are placed vertically, the gravity-oriented magnet also results in the most sensitive range of measurement. The designed smart rocks will be prototyped as a concrete encasement in applications.

During this quarter, the effect of resetting deposits on the magnetic field near the Gasconade River Bridge site was tested. To this end, a hole was excavated near a bridge pier, a magnet was placed at the bottom of the hole and covered by deposits of different heights, and the intensity of the magnetic field of the magnet and other ferromagnetic substances were measured at two fixed locations. As expected, the resetting deposits have little effect on the magnetic measurement. In addition, whether steel reinforcement in a bridge pier would affect the magnetic measurement was also investigated. Based on the field tests, no obvious change was observed in the orientation of a magnet when placed near a bridge pier with steel reinforcement.

I - TECHNICAL STATUS

I.1 ACCOMPLISHMENTS BY MILESTONE

In this quarter, bridge and river data were collected to determine the critical condition of water flow for the incipient motion of cohesionless particles. Specifically, the critical shear stress or the critical velocity was calculated following the guidelines in HEC18 and HEC 23. The critical velocity of water flow for the incipient motion of cohesionless particles and the critical shear stress of cohesionless particles as well as the riprap size were evaluated to determine the size or density of smart rocks for each bridge site. The size and configuration of the smart rock were finalized. The smart rocks were prototyped as concrete encasements. In addition, tests were conducted to verify that resetting deposits in a refilled scour hole have no effect on the magnetic field measurement and smart rocks would not be attracted and attached on any bridge pier with significant steel reinforcement during the normal operation of smart rocks. Finally, the plan for a mock-up test on the bridge deck with magnetic field measurements is developed for the US63 Gasconade River Bridge.

Task 1.1 Motion of Smart Rocks under Various Flow Conditions - Critical Flow Conditions Summarized for Various Cases

A. Criteria of Incipient Motion of Rocks

The incipient motion of a single particle is likely activated by the threshold condition between erosion and sedimentation of the rock. Based on the river geometrics, the hydraulic conditions, the channel bed shapes, the bed sediment size, and the viscous properties of the bed sediment materials, different empirical criteria can be used to evaluate the incipient motion of a sediment particle. According to HEC18, the critical velocity V_c is referred to as the velocity at which cohesionless particles begin to move. Similarly in HEC 18, the critical shear stress τ_c is referred to as the shear stress that represents the initiation of motion for cohesionless particles. In addition, the HEC 23 provided a formula for rock riprap sizing d_{50} on a channel bed around bridge piers. These approaches were the empirical equations obtained through model experiments and may have different application limitations. In what follows, three criteria in terms of the critical velocity of a rock, the critical shear stress of a rock, and the riprap sizing method was discussed and compared according to HEC18 and HEC 23.

A1. Critical velocity V_c

The critical velocity at which cohensionless particles (e.g., sands and gravels) begin to move can be determined by Eq. (12) in HEC 18 (3rd version):

$$V_c = \frac{K_s^{1/2}\left(S_s - 1\right)^{1/2} d^{1/2} y^{1/6}}{n} \tag{1}$$

where V_c is the critical velocity in m/s; K_s is a dimensionless Shields parameter (=0.047 for sands, 0.030 for gravels, and 0.052~0.054 for cobbles and boulders) used to calculate the initiation of motion of sediment in a fluid flow; S_s is the specific gravity of riverbed particles; d

represents the size of a single particle (smart rock in this study) in m; y is the depth of water flow in m; and n is the Manning's roughness coefficient.

A2. Critical shear stress τ_c

The critical shear stress τ_c for the initiation of motion for cohesionless soil particles can be estimated using the Shields relation:

$$\tau_c = K_s(\rho_s - \rho_w)\,\mathrm{gd} \tag{2}$$

where τ_c is the critical shear stress of a particle in lb/ft^2 (N/m^2); ρ_s is the particle mass density, slugs/ft^3(kg/m^3); ρ_w is the mass density of water (=1.94 slugs /ft^3 or 1,000 kg/m^3 for fresh water); and g is the gravitational acceleration (=32.2 ft/s^2 or 9.81 m/s^2). The shear stress at any point of river bed is determined by hydraulic characteristics. For example, the local shear stress in the vicinity of a bridge pier or abutment can be calculated by:

$$\tau_{local} = \left(\frac{nV_{local}}{K_u}\right)^2 \frac{\gamma_w}{y^{1/3}} \tag{3}$$

where τ_{local} is the local shear stress in lb/ft^2 (N/m^2); V_{local} is the local velocity in ft/s (m/s); γ_w is the density of water (=62.4 lb/ft^3 or 9800 N/m^3 for fresh water); K_u is a conversion factor (=1.486 for U.S. customary units and 1 for SI units).

By equating τ_c to τ_{local}, the particle size d can be calculated from Eq. (2) as a function of the basic properties of water flow and particles. In general, the mass density of quartz particles of 2650 kg/m^3 does not vary significantly with temperature and is assumed constant in most calculations. Thus, for a certain condition of smart rocks, the mass density can also be designed as the constant value 2650 kg/m^3 and the size is the only unknown to be calculated.

A3. Riprap size design

The riprap piled up around the footing of the pier is a common measure for local scour protection. In the Design Guideline 8 of HEC 23 (version 2), the rearranged Isbash formula can be used to solve the diameter of the riprap on a channel bed (in meters for fresh water):

$$D_{50} = \frac{0.692(KV)^2}{2g\left(S_s - 1\right)} \tag{4}$$

where D_{50} is the median stone diameter, m; K is the coefficient for pier shape (=1.5 for round-nose piers and 1.7 for rectangle piers); V is equal to the average channel velocity, m/s, multiplied a coefficient of 0.9 for a pier near the river bank in a straight uniform stream and 1.7 for a pier in the main current of flow around a bend; S_s is the specific gravity of riprap (normally 2.65); g is 9.81m/s^2. The size of the smart rock with the density of 2650 kg/m^{3}can be estimated from Eq. (4) given the velocity of the flow around the pier.

B. Incipient Motion at Various Bridge Sites

Four bridges over rivers or creeks were selected for validation testing of the monitoring technology with passive smart rocks. Two of them located in California are Highway 1 over Waddell Creek (Br. No. 36-0065) and Highway 9 over Kings Creek (Br.No.36-0054). The other

two bridges located in Missouri are US63 Highway over the Gasconade River and I-44 Highway over Roubidoux Creek.

Since the critical velocity of a rock is derived as its local shear stress reaches a critical value, the first two criteria are equivalent. As such, the following calculations are focused on the two criteria based on the critical velocity and the riprap size.

B1. Highway 1 over Waddell Creek (Br. No. 36-0065)

The bridge is located approximately 17 miles north of the City of Santa Cruz in Santa Cruz County. Built in 1947, the 4-span structure as shown in Figure 1 is 180.8 ft long and 31.7 ft wide. Continuous reinforced concrete (RC) T-girders are supported on RC piers and seat-type abutments. All the piers and abutments are founded on cast-in-drilled-hole (CIDH) concrete piles, which is reinforced in the upper portion and cast in tapered steel shells in the lower portion.

Figure 1 Highway No.1 Waddell Creek Bridge

In the upstream of the bridge, the terrain is dominated by small mountain ranges that flank both sides of the creek. In the downstream of the bridge, the channel alignment changes with flow intensity as it flows through the beach (loose, coarse sand) towards the Pacific Ocean.

In February of 2000, high flows from a storm caused severe erosion to the upstream channel banks of the south roadway approach, extending into the embankment at Abutment 1. The high flows also exposed some piles at Pier 2 up to 9 ft. Rock slope protection (0.7 to 1 m in diameter) was placed in March of 2000 along the eroded sections of the roadway embankments and channel banks. Since then, this bridge has been classified as scour critical. In order to estimate its scour potential, hydraulic parameters (flow skew, tidal influence, flow contraction, and pressure flow) were obtained from an advanced 2-D hydraulic model established by Caltrans.

The 100-year flood discharge (Q_{100}) in the channel was estimated from the regional flood-frequency equation based on the historical gaga data from USGS. It was calculated to be 162 m^3/s and rounded up to 170 m^3/s in this study. During the 100-year flood, the high water elevation (HWEL) reached 2.865 m, which is well below the bottom of girder elevation (El = 4.145 m). Therefore, no submersed condition existed and no pressure flow occurred. The uncontrolled tide from the Pacific Ocean has no effect on the flow elevation at the bridge site.

The flow depth (y) and velocity (V) in the directly upstream of various piers obtained from the 2-D analysis model are listed in Table 1.

Table 1 Hydraulic Parameters at Various Bents

Bent No.	2	3	4
y (m)	3.566	2.012	0.152
V (m/s)	2.286	3.048	1.585

The materials in channel bed vary from coarse sands to large cobbles. Specifically, mostly coarse sands were noted in the vicinity of the bridge, mostly small pebbles were found in the further upstream of the bridge, and pebbles and/or cobbles were noted in the downstream of the bridge. The sampled size distribution in the downstream of the bridge gave D_{50}=3.658 cm and D_{95}=10.363 cm.

The Manning's roughness "n" value was 0.02 for the channel and beach areas, 0.04 for the grassy banks, 0.045 for the large rock slope protection zone, and 0.10 for the bank sections lined up with small trees.

It was concluded by Caltrans that Bent 2 will be laterally unstable during the anticipated 100-year flood event due to excessive pile exposure. Scour at Bents 3 and 4 should not have any instability issues. Therefore, the hydraulic parameters at Bent 2 were selected to estimate the size and density of smart rocks in this study.

Based on critical velocity Eq. (1) was used to estimate the density of a smart rock with the following parameters: K_s = 0.052 for fine cobbles from the USGS Scientific Investigations Report 2008-5093; $S_s = \rho_s/1000$ where ρ_s is the mass density of smart rocks in kg/m^3; g = 9.81 *m/s*^{2}; d = 0.25 m for smart rocks based on the required space for magnet embedment; $V_c = V$ = *2.286 m/s* at Bent 2; y = 3.566 *m* at Bent 2; and $n = 0.041 d^{1/6} = 0.0325$. That is,

$$2.286 = \frac{0.052^{1/2}\left(\frac{\rho_s}{1000}-1\right)^{1/2} 0.25^{1/2} 3.566^{1/6}}{0.0325}, \quad \rho_s = 1278 kg/m^3$$

Based on riprap size The smart rocks used to monitor effectiveness of the RSP will be deployed at the toe of Abutment 5, using the flow velocity at Bent 4. The diameter of the rocks on a channel bed is determined by Eq. (4) with the following parameters: D_{50} = 0.25 m; K=1.7 for a rectangle pier; V = 1.585 m/s at Bent 4; Ss = ρ_s/1000 in kg/m^3; and g = 9.81 m/s^2. That is,

$$0.25 = \frac{0.692(1.7\times 1.585)^2}{2\times 9.81\left(\frac{\rho_s}{1000}-1\right)}, \quad \rho_s = 2024 kg/m^3$$

B2. Highway 9 over Kings Creek (Bridge No.36-0054)

As shown in Figure 2, the Kings Creek Bridge is a 2-span structure that carries Highway 9 traffic in Santa Cruz County over the Kings Creek. It is located at the apex of a bend in the channel with the main channel flowing under Span 2.

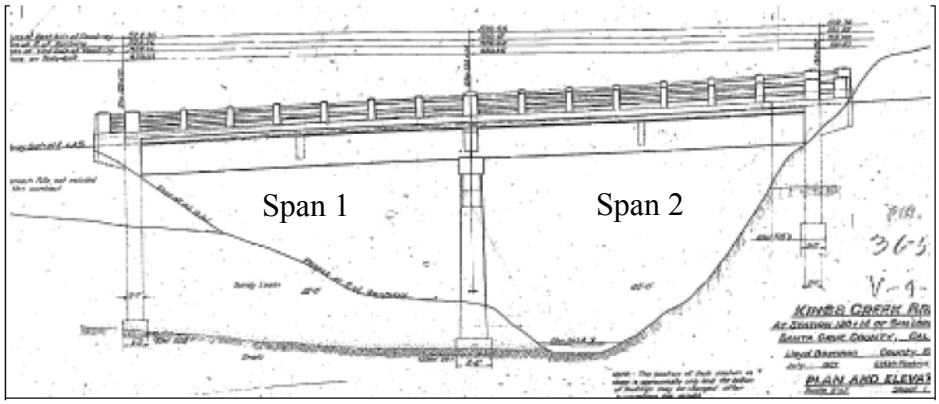

Figure 2 Schematic view of Kings Creek Bridge No.36-0054

This bridge was classified as scour critical in 2004; its foundations were determined to be unstable for assessed or calculated scour conditions. The footing pads at Bent 2 for both columns were found to be severely exposed. In addition to the exposure of the bent footings, a large section of the downstream right bank (looking in the downstream direction) near the bridge is severely eroded. In order to conduct the assessment of the scour condition, a 2D hydraulic model of the flow around the bend where the bridge crossing is located was established and analyzed by Caltrans to determine various hydraulic parameters at the bridge site.

The 100-year flood discharge (Q_{100}) was estimated to be 76.693 m^3/s from STREAMSTATS, a web-based program developed by the USGS. The flow depth and flow velocity corresponding to the 100-year flood at Bent 2 is unknown. However, the threshold bed-shear stress and velocity that would increase erosion were provided as listed in Table 2.

Table 2 Threshold Values

Hydraulic Parameter	Threshold values that would increase erosion
Bed Shear Stress	> 5 N/m^2
Velocity Magnitude	> 0.15 m/sec
HWEL	> 0.15 m

The critical velocity criterion was applied to estimate the density of smart rocks given d = 0.25 m and the hydraulic parameters selected according to Table 2. Specifically, V = 0.2 m/s and HWEL (y) = 0.18 m were considered at Bent 2. Again, K_s = 0.052 and n = $0.041d^{1/6}$=0.0325; Ss = $\rho_s/1000$ where ρ_s is the mass density of smart rocks in kg/m^3. The density of smart rocks is estimated by:

$$0.2 = \frac{0.052^{1/2}\left(\frac{\rho_s}{1000}-1\right)^{1/2} 0.25^{1/2} 0.18^{1/6}}{0.0325}, \quad \rho_s = 1006\, kg/m^3$$

B3. US63 Gasconade River Bridge

The bridge over the Gasconade River on US Highway 63 is located approximately 5.5 miles southeast of Vienna in Maries County, MO. Built in 1970's, it is a 12-span concrete-girder

structure as schematically shown in Figure 3. The main flow goes between Bents 4 and 5 during dry seasons. During a flood season, Bent 4 could be potentially subjected to severe contraction scour and local scour, threatening the safety of the bridge. The 100-year flood discharge (Q_{100} = 146000 *cfs* = 4234 m^3/s) in the channel was estimated from the historical data recorded from the USGS gage station at Jerome, MO (gage No. 06933500).

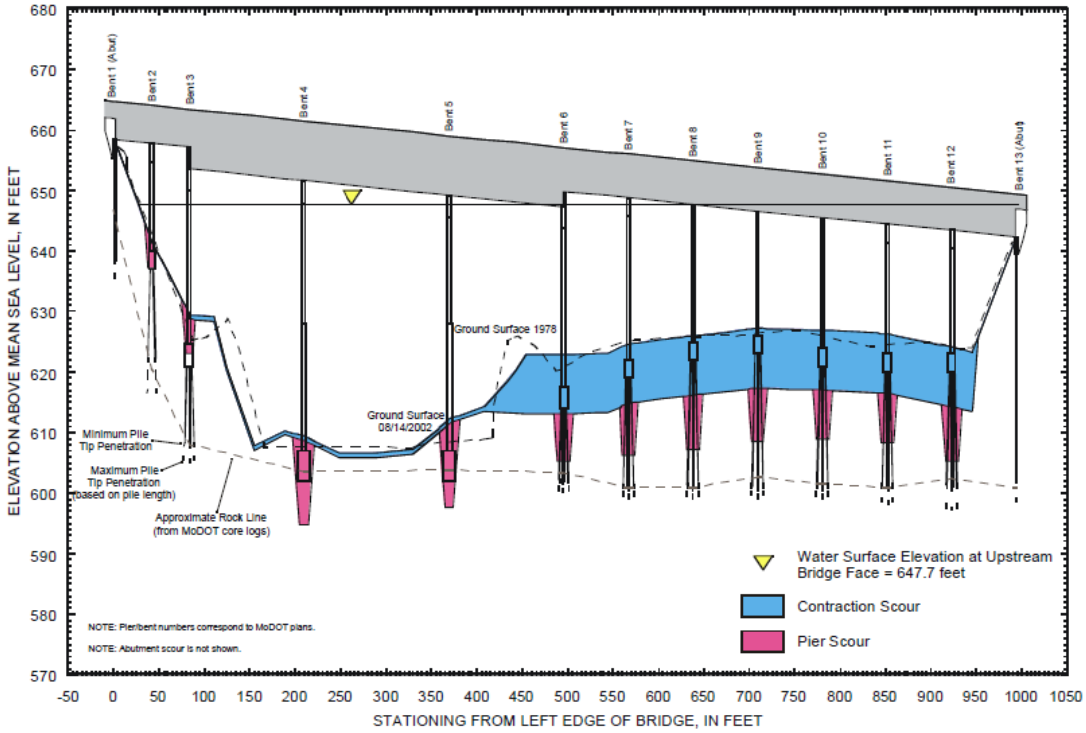

Figure 3 Scour Condition of the Gasconade River Bridge

The average flow velocity at the bridge site was estimated by dividing the 100-year discharge by the cross sectional area of the channel. Based on the as-built bridge drawings and flow elevations shown in Figure 3, the cross sectional area (A) was estimated to be 36544 ft^2 (3395 m^2). Thus, the average channel velocity $V_{average} = Q_{100}/A$ = 1.218 *m/s*. The velocity directly in the upstream of the bent 4 was then calculated by multiplying the average channel velocity by a coefficient of 1.7 for a pier in the main current of flow around a bend. The flow depth at Bent 4 is approximately 40 ft (12.192 m) estimated from Figure 3. Once again, the diameter of smart rocks was taken to be 0.25 m. Therefore, the density of smart rocks can be determined as follows using the critical velocity criterion.

$$1.218\times 1.7 = \frac{0.052^{1/2}\left(\frac{\rho_s}{1000}-1\right)^{1/2} 0.25^{1/2} 12.192^{1/6}}{0.0325}, \quad \rho_s = 1151 kg/m^3$$

B4. I-44 Roubidoux Creek Bridge (Bridge No.L0039)

The Interstate I-44 over the Roubidoux Creek near Waynesville, MO is located about 12 miles South of Crocker in Pulaski County. From the bridge drawings provided by MoDOT, this bridge has 10 spans with the main flow going between Bents 5 and 7 as shown in Figure 4. The pier at

Bent 6 may be scour critical. Since there is no documented record for the 100-year flood discharge near the bridge site, the maximum discharge and flow depth (Q_{max} = 18200 ft/m^3 = 515.4 m^3/s and y=18.70 ft= 5.70 m) recorded at the USGS gage station (USGS 0698300, Roubidoux Creek above Fort Leonard Wood, MO) during the flood event in August, 2013, were used in calculation. The cross sectional area (A) during the flood event was estimated to be 11703 ft^2 (1087 m^2) from the bridge drawings. Therefore, the average channel velocity $V_{average}$ = Q_{max} /A = 0.474 m/s, and the velocity directly in the upstream of Bent 6 was estimated by multiplying the average channel velocity by a coefficient of 1.7.

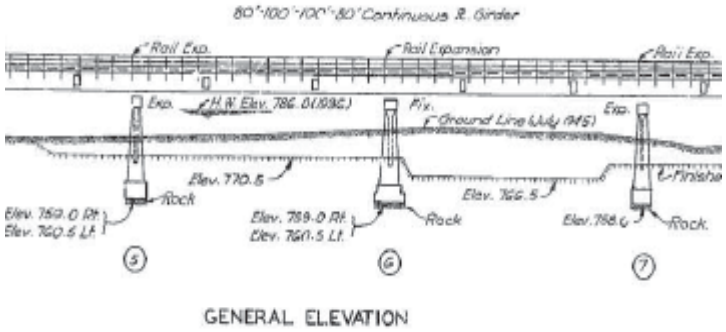

Figure 4 Schematic view of I-44 Roubidoux Creek Bridge at Bents 5-7

Once again, the diameter of smart rocks was kept to be 0.25 m. Therefore, the mass density of smart rocks can be determined based on the critical velocity as follows.

$$0.474\times 1.7 = \frac{0.052^{1/2}\left(\frac{\rho_s}{1000}-1\right)^{1/2} 0.25^{1/2} 5.70^{1/6}}{0.0325}, \quad \rho_s = 1030\, kg/m^3$$

Task 1.2 Design Guidelines of Smart Rocks - Draft Design Guidelines Completed & Sent out for Review

Based on the analyses in Subtask 1.1 and the conceptual study of smart rocks in the previous phase, the following draft design guidelines of smart rocks are proposed. They include three main sections: Introduction, Design Considerations, and Design Procedure.

A. Introduction

Smart rocks are natural rocks or concrete encasements with embedded objects to facilitate remote measurements of their spatial locations. They are passive when the embedded objects are permanent magnets and the magnets are remotely located with one or several magnetometers, and active when the embedded objects are sensors and communication devices and the sensors are located from a remote measurement station through wireless communication. When deployed near a scour critical bridge pier, smart rocks are displaced as their underlying deposits are eroded away. Therefore, properly-designed smart rocks can provide the critical information about the onset movement of riprap slope protection. If the motion of smart rocks can be controlled such that the rocks remain at the bottom of a developing scour hole near the bridge pier, the smart

rocks can also provide critical information about the maximum scour depth, which is the most important parameter in bridge engineering and design for scour effect.

B. Design Considerations

Smart rocks are designed to meet two requirements: 1) facilitate remote measurement for rock localization and 2) ensure automatic movement to the bottom of a scour hole to be monitored. The size of smart rocks is often constrained by the minimum size of embedded objects, such as permanent magnets, that are required for sufficient localization accuracy and measurement distance. The size and density of smart rocks must be selected such that the rocks can always stay at the river bed, overcome water current and roll down the slope of a scour hole, and remain at the bottom of the hole. Therefore, the density of smart rocks should range from that of water and that of rocks used in riprap slope protection.

To overcome water current and roll down the slope of a scour hole, the size and density of smart rocks highly depend on the critical velocity of water flow and the water depth at a bridge site. The critical velocity of water flow is defined as the velocity at which deposits at the river bed begin to move or when the local shear stress of deposits exceeds its critical value. The water depth represents the effect of gravity on the movement of smart rocks, which affects the critical velocity of water flow.

For simplicity, the equation for the critical velocity of water flow in HEC 18 and the equation for the riprap size in scour protection in HEC 23 are referenced in the determination of the size and density of smart rocks. The two equations in SI units are rewritten as follows:

$$d = \frac{(nV_c)^2}{K_s y^{1/3}\left(S_s - 1\right)} \text{ and } D_{50} = \frac{0.692(KV)^2}{2g\left(S_s - 1\right)} \tag{5}$$

where d represents the size of a smart rock in m;
n is the Manning's roughness coefficient;
V_c is the critical velocity of flow in m/s;
K_s is a dimensionless Shields parameter related to the initiation of motion of smart rocks (0.052~0.054 for cobbles and boulders);
$S_s = \rho_s/1000$ where ρ_s is the mass density of smart rocks in kg/m^3;
y is the depth of water flow in m;
D_{50} is the median diameter of smart rocks in m;
K is the coefficient for pier shape (1.5 for round-nose piers and 1.7 for rectangle piers);
V is equal to the average channel velocity, m/s, multiplied by a coefficient of 0.9 for a pier near the river bank in a straight uniform stream or 1.7 for a pier in the main current of flow around a bend; and
g is the gravitational acceleration in m/s^2.

C. Design Procedure

A 3-step design procedure for the selection of the size and density of smart rocks is described as follows.

Step 1: Determine hydraulics parameters near a bridge site. The flow velocity in the channel at a bridge site and the water depth directly in the upstream of scour critical piers, corresponding to a 100-year flood, are two most important parameters needed for the selection of smart rock size and density. They can often be found from hydraulic studies by the United States Geological Survey (USGS) or Federal Emergency Management Agency (FEMA).

When no hydraulic studies are available near a bridge site, the flow discharge from a recent flood event and its corresponding water depth are first estimated from the data collected at any USGS gage station deployed at the upstream or downstream of the bridge site. Considering no water loss, the flood discharge at the bridge site is assumed to be equal to that in the upstream or downstream of the bridge site. The average channel velocity can then be estimated by dividing the flood discharge by the flow cross section, which in turn depends on the water depth at the bridge site. For a given water depth, the flow cross section can be estimated based on the as-built bridge drawings or a site visit with necessary measurements. Next, the local velocity at a scour critical bridge pier is determined by multiplying the average channel velocity by an amplification factor depending on the shape of river at the bridge site, the location of the pier (in main channel or close to the river bank), and the shape of the pier. Finally, the relationship between the local velocity and water depth can be established for sensitivity analysis.

Step 2: Constrain the size and density of a smart rock. Eq. (5) is applied to guide the selection of the size and density of a smart rock. With the local velocity and water depth from Step 1, the size of a smart rock can be related to the density of the rock in an inversely proportional relation. In other words, the larger a smart rock, the lighter the rock for given local velocity and water depth. In practice, either the size or density of a smart rock can be estimated from application needs. For example, the minimum dimension of a magnet to be embedded in a smart rock to meet the required localization accuracy and measurement distance can be referenced in the selection of rock size (e.g. > 20 cm). The density of the smart rock can then be determined correspondingly. Alternatively, the density of a smart rock can be considered to be same as that of natural rocks (2,650 kg/m^3), particularly when the smart rock is deployed to monitor the effectiveness of a riprap slope protection strategy. However, the size corresponding to the density of natural rocks is too small in general. Therefore, smart rocks should be sized first before their density is determined from the critical flow velocity and riprap sizing equations.

Step 3: Finalize the design of smart rocks. After the size and density of smart rocks have been estimated in accordance with the incipient motion of the rocks, the size and density must be modified by a design factor (1.2~1.5) that accounts for any potential errors associated with the estimation of hydraulic data and the use of empirical equations. By considering the design sensitivity to the flow velocity and water depth at the bridge site and the physical constraint on the size and density of smart rocks, several choices of smart rocks are determined. The final selection of the size and density is made by rounding up their calculated numbers and easing the deployment and fabrication of smart rocks, such as the use of standard mold sizes for the casting of concrete encasement.

Task 2.1 Final Design of Smart Rocks

The final design of smart rocks does not only depend on the hydraulic condition they are

subjected to, but also on the intensity of magnetic fields they can generate at a required measurement distance. The field intensity is significantly affected by the size and orientation of the magnets encased in the smart rocks.

A. Size and Density

Smart rocks will be deployed in the river around a bridge pier to measure the maximum scour depth or mixed with natural rocks to form a riprap countermeasure and monitor the effectiveness of the riprap protection. The hydraulic condition of a smart rock was taken into account in the estimation of the rock size and density in Subtask 1.1. Due to deployment convenience and standard mold sizes for the concrete casting of round encasements, the diameter of smart rocks was taken to be 0.25 m. The initial mass density of the smart rocks can then be determined from the local flow velocity and water depth at various bridge sites as discussed in Subtask 1.1. However, due to variability in hydraulic parameters as a result of potential climate change and the change in river condition, the calculated mass density from the critical velocity should be increased by 1.2 or 1.3 times in order to prevent the deployed smart rocks from being washed away, depending on the available hydraulic data at bridge sites.

Specifically, for *Highway 1 Waddell Creek Bridge,* a design factor of 1.2 was considered since a detailed 2D hydraulic model was developed by Caltrans to derive the hydraulic parameters at this site. Therefore, the density of smart rocks should be 1.2×1278 = *1530 kg/m*^{3}, which is still lower than 2024 *kg/m*^{3} that was determined for riprap sizing. For all other bridges*,* a larger design factor of 1.3 was considered due to insufficient information on the local hydraulic data at these sites. Therefore, the density of smart rocks should be 1.3×1006 = *1308 kg/m*^{3} for *Highway 9 Kings Creek Bridge*, 1.3×1151 = *1496 kg/m*^{3} for *US63 Gasconade River Bridge*, and 1.3×1030 = *1339 kg/m*^{3} for I-44 *Roubidoux Creek Bridge*. For easy fabrication, the target density of smart rocks was finally taken to be *1530 kg/m*^{3} for a given diameter of *0.25 m*.

B. Internal Configuration

The magnetic field of a permanent magnet highly depends on the orientation of the magnet. For example, the intensity at two poles of the magnet is twice as much as that at its equator. In practical applications, the magnetic field of a smart rock with an embedded magnet is measured from a magnetometer that is stationed either on the river bank or on the bridge deck.

When a magnetometer is set on the river bank, the two poles of a magnet should be aligned with the Earth's magnetic field for maximum sensitivity or oriented vertically. In the former case, the smart rock with the magnet was referred to as an automatically pointing south system (APSS) as detailed in Figure 5. The advantage of the APSS monitored along the river bank is that the measurement station can be located in South or North pole of the magnet, which facilitates the rapid convergence of the APSS localization algorithm with high accuracy. The disadvantage of the APSS is that the direction of the magnet is easy to be affected by strong ferromagnetic substances in the river. To avoid the direction variation by surrounding ferromagnetic substances, the north pole of the magnet can be faced to the sky. In this case, however, the measurement for maximum sensitivity is restricted to one side of the magnet, which may reduce the accuracy of rock localization.

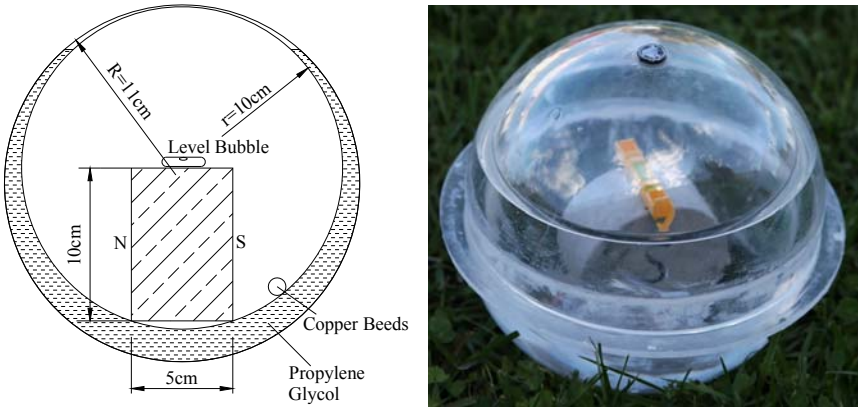

Figure 5 APSS Model of Smart Rocks

When a magnetometer is set on the bridge deck, the two poles of the magnet should face to the sky and ground for better direction alignment in magnetic field measurement due to several reasons. First of all, the strongest magnetic field of a magnet can be found at its two poles, which is in good alignment with the vertical sensor of the magnetometer from the bridge deck. Secondly, the direction of the magnet is less affected by surrounding ferromagnetic substances, which ensures stable and repeatable measurements over time. Finally, the gravity-oriented direction of the magnet considerably reduces the degree of freedom in the localization algorithm. Furthermore, the south pole of the magnet should be faced up or to the bridge deck for larger intensity of the combined magnetic field of surrounding ferromagnetic substances and the magnet since the four bridges are located in northern hemisphere. In this case, the smart rock is referred to as Automatically Pointing to Upward System (APUS) as shown in Figure 6.

(a) Schematic View (b) Propotype Smart Rock (c) Balanced Magnet

Figure 6 APUS Model of Smart Rocks

C. Design Details

A smart rock consists of a cylindrical magnet placed inside an organic glass ball (inside ball), an outside organic glass ball, liquid filled in between the two balls, and a concrete shell encasement. As shown in Figure 6 (with no concrete encasement), the magnet is 10 cm in diameter and 5 cm in height. The side face at the north pole is glued to the surface of the inside ball with a radius of *r*. The outside ball has a radius of *R*. The inside ball with the magnet is designed to stably float

inside the outside ball. Therefore, the magnet in the APUS will always point to the sky to keep the fixed orientation permanently.

Diameter Selection: The selection of ball diameter depends upon three factors: commercial availability of casting molds for two halves of a concrete ball, smart rock size, and floating requirement of the inside ball with negligible friction. To ensure that the inside ball can float in the liquid, the average density of the inside ball with the embedded magnet and other components must be slightly less than that of the liquid. To start with, a value of d = 20 cm was considered. In this case, the mass of the inside ball is equal to the sum of the magnet (3.06 kg), organic glass ball and copper beads (total 0.5 kg), and glue and level indicator (negligible). That is, $\rho_0(\pi)(0.2)^3/6 = 3.06+0.5$ or $\rho_0=850$ kg/m^3, which is less than water density (1000 kg/m^3). Therefore, an inner diameter of 20 cm is a viable choice for the inside ball. The inner diameter of the outside ball can be approximately selected to be 21 cm, which will leave sufficient spacing for lubrication liquid between the inside and outside balls.

Liquid Selection: The liquid between the inside and outside balls must be selected such that the inside ball with the magnet can always float without inducing any notable friction force on the inside ball as it rotates inside the outside ball. For a 20-cm-diameter inside ball, the liquid density must exceed 850 kg/m^3. Although water is a viable candidate in terms of density and nontoxicity requirements, water does not provide sufficient lubrication between the two balls. Lubrication oil is good for minimum friction but insufficient in mass density of the inside ball floating requirement. Consequently, propylene glycol with a mass density of 1040 kg/m^3 is chosen for satisfactory lubrication and nontoxicity requirements.

D. Effect of Deposit Resetting on Magnetic Field

In practice, scour hole develops due to deposit erosion but may be refilled over time. The smart rocks rolling down to the bottom of the scour hole may be covered by the refilling deposits. Whether deposit resetting affects the measurement of magnetic field was investigated at the Gasconade River Bridge site.

As shown in Figure 7, a 1-m deep hole was excavated approximately 10 m away from the bridge pier. A magnet was first wrapped with a plastic bag that was tied afterward with a rope, and then placed into the bottom of the hole. The rope was used to pull the magnet out of the refilled hole after the test was over. The two sensors of a magnetometer were fixed on wood poles (F1 and F2) on two sides of the hole and the magnetometer was set in between the two sensors. Another wood pole F3 placed next to the magnet was marked in 0.5 m interval up to 1.5 m to measure the height of the refilling deposits. As indicated in Figure 8, the measurements were taken first with no deposits, then with the excavated soils refilled to the 0.5 m and 1.0 m marks, and finally with additional deposits piled up to 1.5 m.

Figure 7 Overall Arrangement of Resetting Tests


(a) 0.0 m


(b) 0.5 m


(c) 1.0 m

(d) 1.5 m

Figure 8 Deposits Refilling to Various Heights

Table 3 lists the measured intensity of magnet's and ambient magnetic fields. It can be seen from Table 3 that the maximum variation of the intensities measured for deposits refilling to various heights is 5 nT and 12 nT at F1 and F2, respectively. These variations are significantly less than 100 nT, the level of intensity change that begins to influence the localization accuracy of the magnet. These variations may be caused by the change in Earth's magnetic field at different times of measurement or by other disturbances on the sensor head in the process of deposits refilling.

Table 3 Intensity at Various Deposit Heights

Deposit Height (m)	Intensity (nT)	
	F1	F2
0.0	50869.82	50731.89
0.5	50875.54	50731.06
1.0	50870.06	50720.78
1.5	50868.90	50718.18

E. Effect of Steel Reinforcement on Smart Rock Operation

Effort was made to keep the magnet faced up during measurements so that the magnet orientation is known *in prior* and the error in magnet localization is minimized. One concern to this effort in practical applications is the potential influence of the ferromagnetic substances in bridge pier or foundation. Therefore, a simple test was carried out to rule out this possibility.

Figures 9 and 10 illustrate that the prototype APUS was placed next to a bridge pier and on the bridge foundation, respectively. The APUS represents a smart rock without concrete encasement. It was verified that the bubble remained in the center of a high-precision level attached on the APUS when placed at least 10 m away from the bridge pier and foundation. It can be seen from Figures 9 and 10 that the bubble slightly deviated from the center of the level, indicating an inclination angle of less than 0.5º and thus little effect on the localization of the APUS.

Figure 9 The Prototype APUS Placed next to a Bridge Pier

Figure 10 The Prototype APUS Placed on a Bridge Foundation

Tasks 2.2 Prototyping of Passive Smart Rocks - Concrete Encasement Cast

The prototype APUS will be cast in a spherical concrete encasement to complete a smart rock for field deployment. The first smart rock as shown in Figure 11 was cast in a 25-cm-diameter mold. The total density of the smart rock is ρ_s=[(0.21^{3}m^3) (850kg/m^3) + (0.25^{3}m^3-0.21^{3}m^3)(2500kg/m^3)] / 0.25^3=1520 kg/m^3, which is appropriate for *Highway 1 Waddell Creek Bridge*, *Highway 9 Kings Creek Bridge* and *I-44 Roubidoux Creek Bridge*. The actual density of 1520 kg/m^3 is close to the target value of 1530 kg/m^3. Therefore, the prototype rock is acceptable for field implementation.

Figure 11 A Prototype Smart Rock

The fabrication process of the prototype smart rock is described here. As shown in Figure 6, a high-precision level indicator with bubble was first glued to the top face (north pole) of a magnet, the bottom face (south pole) of the magnet was glued to the wall of half of a spherical ball with attached copper beads near the magnet as balanced weights, and the other half of the spherical ball was attached and sealed to complete an inside ball. The complete inside ball was then placed in half of a larger spherical ball and covered and sealed by the other half to complete the outside ball. Next, a 1-cm-diameter hole was drilled on the outside ball and propylene glycol liquid was injected into the outside ball until the inside ball completely floated and the top of the inside ball was in contact with the outside ball to avoid a large drift of the inside ball. Finally, the injection hole was sealed by a small piece of plastic with adhesives. Figure 6(b) shows a prototype APUS.

Task 3.1 Time- and Event-based Field Measurements - Field Tests Completed & Reported

This task will not start till the 3rd quarter.

Task 3.2 Visualization Tools for Rock Location Mapping over Time - Software Completed & Tested

This task will not start till the 5th quarter.

Task 4 Technology Transfer, Report and Travel Requirements - Quarterly Report Submitted, Travel Completed, or Meeting Conducted

The 2st quarterly report is being submitted.

I.2 PROBLEMS ENCOUNTERED

In this quarter, field tests were delayed due to weather condition in March. However, Missouri Department of Transportation helped the research team get the mock-up field tests done in April.

I.3 FUTURE PLAN

The following task and subtasks will be executed during the next quarter.

Tasks 2.2 Prototyping of Passive Smart Rocks - Concrete Encasement Cast

Based on the final design of smart rocks, concrete encasement will be cast for final deployment at four bridge sites.

Task 3.1 Time- and Event-based Field Measurements - Field Tests Completed & Reported

The field tests at four bridge sites will be conducted to validate the localization of smart rocks. The mock-up field test procedure on the bridge deck was practiced at the Gasconade River Bridge on April, 1 2015. The data process is now under way.

Task 3.2 Visualization Tools for Rock Location Mapping over Time - Software Completed & Tested

This task will not start till the 5th quarter.

Task 4 Technology Transfer, Report and Travel Requirements - Quarterly Report Submitted, Travel Completed, or Meeting Conducted

The 3nd quarterly report will be prepared and submitted. Towards the end of April or Early May, the 2nd meeting with Technical Advisory Council (TAC) will be organized to discuss the progress in the first 6 months. Feedbacks will be sought and considered in the execution of future tasks.

.

II – BUSINESS STATUS

II.1 HOURS/EFFORT EXPENDED

The planned hours and the actual hours spent on this project are given and compared in Table 4. In the second quarter, the actual hours are less than the planned hours, leading to an actual cumulative hour of approximately 28% of the planned hours. The cumulative hours spent on various tasks by personnel are presented in Figure 12.

Table 4 Hours Spent on This Project

	Planned		Actual	
	Labor Hours	Cumulative	Labor Hours	Cumulative
Quarter 1	945	945	176	176
Quarter 2	752	1697	294	471
Quarter 3				
Quarter 4				
Quarter 5				
Quarter 6				
Quarter 7				
Quarter 8				

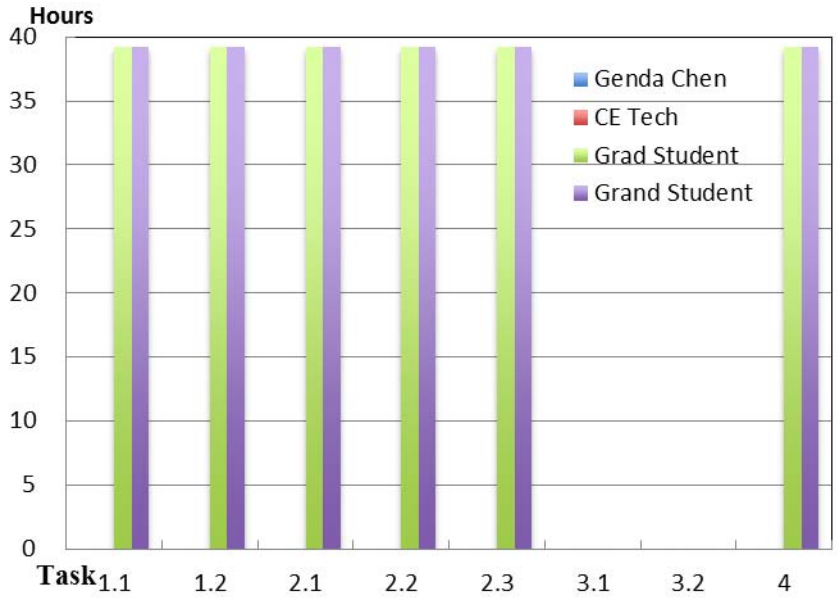

Figure 12 Cummulative Hours Spent on Various Tasks by Personnel

II.2 FUNDS EXPENDED AND COST SHARE

The budgeted and expended OST-R funds accumulated by quarter are compared in Figure 13. Approximately 45% of the budget has been spent till the end of second quarter. The actual cumulative expenditures from OST-R and MS&T/MoDOT are compared in Figure 14. The expenditure from OST-R is less than the combined amount from the MS&T and MoDOT.

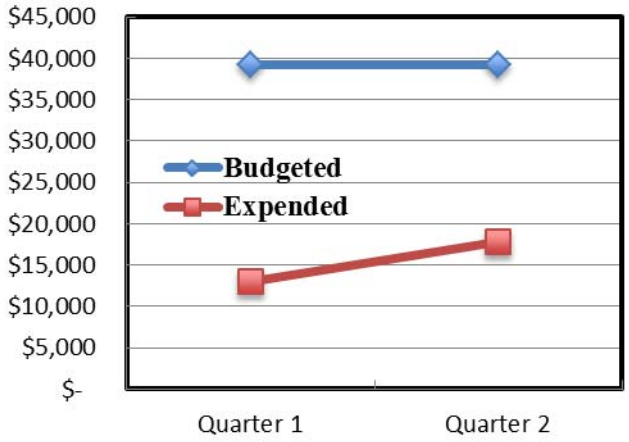

Figure 13 Comparison of OST-RBudget and Expenditure Accumulated by Quarter

Figure 14 Cummulative Expenditures by Sponsor